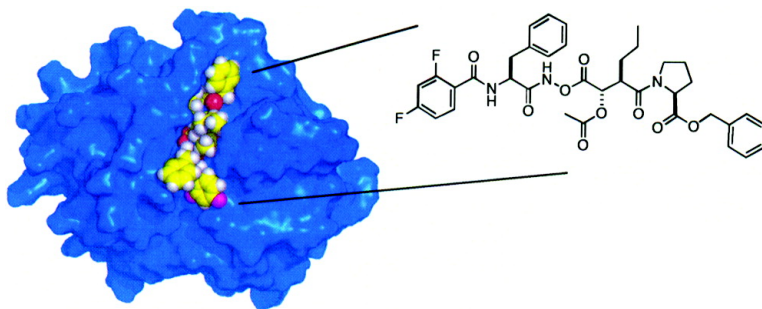


Strategy in Inhibition of Cathepsin B, A Target in Tumor Invasion and Metastasis

In Taek Lim, Samy O. Meroueh, Mijoon Lee, Mary Jane Heeg, and Shahriar Mobashery

J. Am. Chem. Soc., **2004**, 126 (33), 10271-10277 • DOI: 10.1021/ja0489240 • Publication Date (Web): 03 August 2004

Downloaded from <http://pubs.acs.org> on April 1, 2009



More About This Article

Additional resources and features associated with this article are available within the HTML version:

- Supporting Information
- Access to high resolution figures
- Links to articles and content related to this article
- Copyright permission to reproduce figures and/or text from this article

[View the Full Text HTML](#)

Strategy in Inhibition of Cathepsin B, A Target in Tumor Invasion and Metastasis

In Taek Lim,[†] Samy O. Meroueh,[†] Mijoon Lee,[†] Mary Jane Heeg,[‡] and Shahriar Mobashery^{*†}

Contribution from the Department of Chemistry and Biochemistry and Walther Cancer Research Center, University of Notre Dame, Notre Dame, Indiana 46556 and Department of Chemistry, Wayne State University, Detroit, Michigan 48202

Received February 25, 2004; E-mail: mobashery@nd.edu

Abstract: Cathepsin B, a cysteine protease, is an important target in fighting cancer. This enzyme has been implicated in enhancing tumor invasiveness and metastasis, therefore inhibitors for cathepsin B are highly sought as potential anticancer and antimetastatic agents. A structure-based design effort was pursued in arriving at a template for inhibition of cathepsin B. Focused compound libraries were synthesized based on this template, which were screened for cathepsin B inhibitory properties. Compound **2**, 1-(2(R)-{1(S)-acetoxy-2-[2(S)-(2,4-difluoro-benzoylamino)-3-phenyl-propionylaminoxy]-2-oxo-ethyl}-pentanoyl)-pyrrolidine-2(S)-carboxylic acid benzyl ester, is the prototype of this novel class of cysteine protease inhibitor that emerged from the search. The molecule modifies the active site of cathepsin B covalently, irreversibly, and efficiently, a process for which the kinetic parameters were evaluated. A set of three judiciously altered variants of compound **2** was also synthesized to explore the details of the proposed mechanism of action by this inhibitor. Compound **2** and its analogues may prove useful tools in reversing the deleterious effect of cathepsin B in fighting cancer.

Malignant tumors have a tendency to invade the surrounding tissue and gain access to the vasculature.¹ The tumor sheds cells into the vasculature, which in turn transports the cells to secondary sites for reestablishment of the tumor. The occurrence of these events, referred to as tumor metastasis, bodes poorly for the patients and leads to death in more than 90% of the cases.² Although processes involved in tumor invasion and metastasis are complex, a prerequisite for these events is the degradation of the extracellular matrix by specific proteases.^{3–8} Cathepsin B, an important cysteine protease of the papain superfamily has been documented to be important in many metastatic tumors.^{9–20} The linking of cathepsin B to tumor

progression and invasion is based on observations that its levels of activity and secretion are increased in tumors.^{9–24} The highest level of cathepsin B activity is seen in the most malignant tumors, and particularly so in cells that are at the invasive edge of these tumor masses.^{25–27} Therefore, cathepsin B is considered an important target in cancer intervention and inhibitors for it are highly sought.^{28–33}

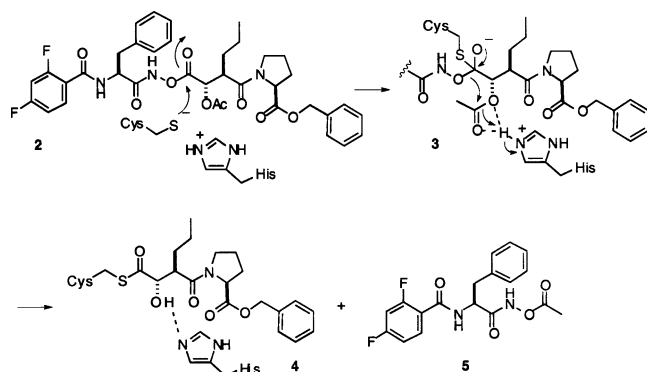
[†] Department of Chemistry and Biochemistry and Walther Cancer Research Center, University of Notre Dame.

[‡] Department of Chemistry, Wayne State University.

- (1) Engers, R.; Gabbert, H. E. *J. Cancer Res. Clin. Oncol.* **2000**, *126*, 682–692.
- (2) Gabbert, H. E.; Meier, S.; Gerharz, C. D.; Hommel, G. *Int. J. Cancer* **1991**, *49*, 203–207.
- (3) Mignatti, P.; Rifkin, D. B. *Physiol. Rev.* **1993**, *73*, 161–195.
- (4) Sloane, B. F.; Elliott, E. *Perspect. Drug Discovery* **1996**, *6*, 12–32.
- (5) Sameni, M.; Moin, K.; Sloane, B. F. *Neoplasia* **2000**, *2*, 496–504.
- (6) Stetler-Stevenson, W. G.; Yu, A. E. *Semin. Cancer Biol.* **2001**, *11*, 143–152.
- (7) Johnsen, M.; Lund, L. R.; Romer, J.; Almholt, K.; Dano, K. *Curr. Opin. Cell Biol.* **1998**, *10*, 667–671.
- (8) Chambers, A. F.; Matrisian, L. M. *J. Natl. Cancer Inst.* **1997**, *89*, 1260–1270.
- (9) Frohlich, E.; Schlagenhaufl, B.; Mohrle, M.; Weber, E.; Klessen, C.; Rassner, G. *Cancer* **2001**, *91*, 972–982.
- (10) Lah, T. T.; Kokalj-Kunovar, M.; Strukelj, B.; Pungercar, J.; Barlic-Maganja, D.; Drobnic-Kosorok, M.; Kastelic, L.; Babnik, J.; Golouh, R.; Turk, V. *Int. J. Cancer* **1992**, *50*, 36–44.
- (11) Krepela, E.; Vicar, J.; Cernoch, M. *Neoplasia* **1989**, *36*, 41–52.
- (12) Poole, A. R.; Tiltman, K. J.; Recklies, A. D.; Stoker, T. *Nature* **1978**, *273*, 545–547.

- (13) Castiglioni, T.; Merino, M. J.; Elsner, B.; Lah, T. T.; Sloane, B. F.; Emmert-Buck, M. R. *Hum. Pathol.* **1994**, *25*, 857–862.
- (14) Benitez-Bribiesca, L.; Martinez, G.; Ruiz, M. T.; Gutierrez-Delgado, F.; Utrera, D. *Arch. Med. Res.* **1995**, *26*, S163–S168.
- (15) Recklies, A. D.; Tiltman, K. J.; Stoker, T. A.; Poole, A. R. *Cancer Res.* **1980**, *40*, 550–556.
- (16) Ohsawa, T.; Higashi, T.; Tsuji, T. *Acta Med. Okayama* **1989**, *43*, 9–15.
- (17) Corticchiato, O.; Cajot, J. F.; Abrahamson, M.; Chan, S. J.; Keppler, D.; Sordat, B. *Int. J. Cancer* **1992**, *52*, 645–652.
- (18) Heidtmann, H. H.; Salge, U.; Abrahamson, M.; Bencina, M.; Kastelic, L.; Kopitar-Jerala, N.; Turk, V.; Lah, T. T. *Clin. Exp. Metastasis* **1997**, *15*, 368–381.
- (19) Hughes, S. J.; Glover, T. W.; Zhu, X. X.; Kuick, R.; Thoraval, D.; Orringer, M. B.; Beer, D. G.; Hanash, S. *Proc. Natl. Acad. Sci. U.S.A.* **1998**, *95*, 12 410–12 415.
- (20) Krepela, E.; Kasafirek, E.; Novak, K.; Viklicky, J. *Neoplasia* **1990**, *37*, 61–70.
- (21) Lah, T. T.; Calaf, G.; Kalman, E.; Shinde, B. G.; Somers, R.; Estrada, S.; Salero, E.; Russo, J.; Daskal, I. *Breast Cancer Res. Treat.* **1996**, *39*, 221–233.
- (22) Campo, E.; Munoz, J.; Miquel, R.; Palacin, A.; Cardesa, A.; Sloane, B. F.; Emmert-Buck, M. R. *Am. J. Pathol.* **1994**, *145*, 301–309.
- (23) Leto, G.; Tumminello, F. M.; Pizzolanti, G.; Montalto, G.; Soresi, M.; Gebbia, N. *Oncology* **1997**, *54*, 79–83.
- (24) Kos, J.; Stabuc, B.; Schweiger, A.; Krasovec, M.; Cimerman, N.; Kopitar-Jerala, N.; Vrhovec, I. *Clin. Cancer Res.* **1997**, *3*, 11 815–11 822.
- (25) Mai, J.; Waisman, D. M.; Sloane, B. F. *Biochim. Biophys. Acta* **2000**, *1477*, 215–230.
- (26) Koblinski, J. E.; Ahram, M.; Sloane, B. F. *Clin. Chim. Acta* **2000**, *291*, 113–135.
- (27) Berquin, I. M.; Sloane, B. F. *Persp. Drug Discov. Design* **1995**, *2*, 371–388.

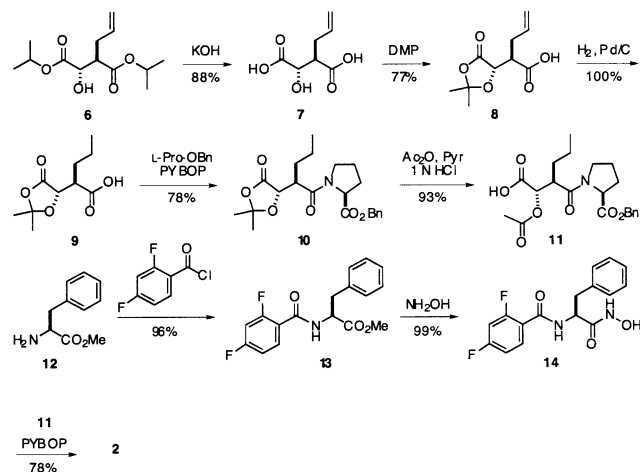
Scheme 1



It is believed that Cys-29 and His-199 exist as an ion pair in the native cathepsin B.^{34–36} Cathepsin B undergoes acylation by its substrates at Cys-29 and the acyl-enzyme species undergoes hydrolysis in the second part of catalysis. We conceived of a strategy in inhibition of cathepsin B by tying up the two catalytic residues in a manner that they would not be available for the catalytic processes. We envisioned that a molecule could be designed such that it would undergo interaction with the reactive Cys-29 thiolate, and in the process it would make a hydrogen bond to His-199, such that it cannot perform its proton transfer function in the normal turnover events of the enzyme. Such a molecule may conceivably result in either a stable acyl-enzyme species or a species en route to the acyl-enzyme entity, either of which could result in irreversible inhibition of cathepsin B.

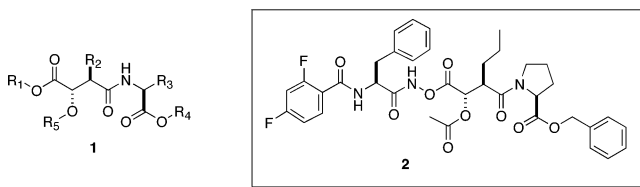
The design process started with the X-ray structure of cathepsin B³² and that of an inhibitor bound to its active site cysteine.³⁷ The original concept went through a number of iterations by extensive use of molecular docking based on a genetic algorithm,³⁸ and several analogues were synthesized and tested in *in vitro* experiments with the purified enzyme. The lead structural template that emerged out of these efforts (**1**) was refined by syntheses of several focused libraries of 80 compounds that created diversity for groups R₁ to R₄ (see structure **1**), which were individually tested for cathepsin B inhibition. The culmination of these efforts was compound **2**. Compound **2** was expected to modify Cys-29 to give species **3** (Scheme 1). Molecular modeling argues that the potential for hydrogen bonding between the acetyl moiety and the protonated His-199 exists and this structure may be stabilized within the active site. Alternatively, species **3** may fragment to give species

Scheme 2



4, which would be expected to hydrogen bond with the unprotonated His-199 and attenuate its basicity. By so doing, *not only the histidine will be a poorer base for promotion of the water molecule for the “second step” of catalysis, but also the hydroxyl moiety that interacts with it is predisposed at the position of the incoming hydrolytic water molecule.* Other strategies in inhibition that tie up catalytic residues in serine-dependent enzymes have been described.^{39–46}

Either species **3** or **4** could account for the mechanism of inhibition by compound **2**, both of which are unprecedented and novel for inhibition of cysteine proteases.^{47,48}



Synthesis of compound **2** is depicted in Scheme 2. 2(R)-Allyl-3(S)-hydroxysuccinic acid diisopropyl ester **6** was prepared from (S)-malic acid diisopropyl ester⁴⁹ and was hydrolyzed to give the diacid **7**. The absolute stereochemistry of compound **7** was determined by X-ray crystallography, and the ORTEP presentation of the crystal structure is given as Supporting Information.

The acetonide group was introduced for protection of the α -hydroxycarboxylic acid (**8**). Catalytic hydrogenation of the allyl group of **8** led to the derivative **9**. Compound **9** was elaborated with L-proline benzyl ester to give **10**. After deprotection of the acetonide, the hydroxyl group was acetylated

- (28) Murata, M.; Miyashita, S.; Yokoo, C.; Tamai, M.; Hanada, K.; Hatayama, K.; Towatari, T.; Nikawa, T.; Katunuma, N. *FEBS Lett.* **1991**, *280*, 307–310.
- (29) Towatari, T.; Nikawa, T.; Murata, M.; Yokoo, C.; Tamai, M.; Hanada, K.; Katunuma, N. *FEBS Lett.* **1991**, *280*, 311–315.
- (30) Xing, R.; Hanzlik, R. P. *J. Med. Chem.* **1998**, *41*, 1344–1351.
- (31) Schaschke, N.; Assfalg-Machleidt, L.; Lassleben, T.; Sommerhoff, C. P.; Moroder, L.; Machleidt, W. *FEBS Lett.* **2000**, *481*, 91–96.
- (32) Greenspan, P. D.; Clark, K. L.; Tommasi, R. A.; Cowen, S. D.; McQuire, L. W.; Farley, D. L.; Duzer, J. H.; Goldberg, R. L.; Zhou, H.; Du, Z.; Fitt, J. J.; Coppa, D. E.; Fang, Z.; Macchia, W.; Zhu, L.; Capparelli, M. P.; Goldstein, R.; Wigg, A. M.; Doughty, J. R.; Bohacek, R. S.; Knap, A. K. *J. Med. Chem.* **2001**, *44*, 4524–4534.
- (33) Otto, H.-H.; Schirmeister, T. *Chem. Rev.* **1997**, *97*, 133–177.
- (34) Lewis, S. D.; Johnson, F. A.; Shafer, J. A. *Biochemistry* **1976**, *15*, 5009–5017.
- (35) Lewis, S. D.; Johnson, F. A.; Shafer, J. A. *Biochemistry* **1981**, *20*, 48–51.
- (36) Polgar, L. *Eur. J. Biochem.* **1975**, *51*, 63–71.
- (37) Yamamoto, A.; Tomoo, K.; Matsugi, K.; Hara, T.; In, Y.; Murata, M.; Kitamura, K.; Ishida, T. *Biochim. Biophys. Acta* **2002**, *1597*, 244–251.
- (38) Morris, G. M.; Goodsell, D. S.; Halliday, R. S.; Huey, R.; Hart, W. E.; Belew, R. K.; Olson, A. J. *J. Comput. Chem.* **1998**, *19*, 1639–1662.

- (39) Liang, T. C.; Abeles, R. H. *Biochemistry* **1987**, *26*, 7603–7608.
- (40) Ringe, D.; Mottonen, J. M.; Gelb, M. H.; Abeles, R. H. *Biochemistry* **1986**, *25*, 5633–5638.
- (41) Miyashita, K.; Massova, I.; Taibi, P.; Mobashery, S. *J. Am. Chem. Soc.* **1995**, *117*, 11 055–11 059.
- (42) Maveyraud, L.; Massova, I.; Birck, C.; Miyashita, K.; Samama, J.-P.; Mobashery, S. *J. Am. Chem. Soc.* **1996**, *118*, 7435–7440.
- (43) Reed, P. E.; Katzenellenbogen, J. A. *J. Med. Chem.* **1991**, *34*, 1162–1176.
- (44) Baek, D. J.; Katzenellenbogen, J. A. *Biochem. Biophys. Res. Commun.* **1991**, *178*, 1335–1342.
- (45) Daniels, S. B.; Katzenellenbogen, J. A. *Biochemistry* **1986**, *25*, 1436–1444.
- (46) Wilmonth, R. C.; Westwood, N. J.; Anderson, K.; Brownlee, W.; Claridge, T. D. W.; Clifton, I. J.; Pritchard, G. J.; Aplin, R. T.; Schofield, C. J. *Biochemistry* **1998**, *37*, 17 506–17 513.
- (47) Powers, J. C.; Asgian, J. L.; Ekici, O. D.; James, K. E. *Chem. Rev.* **2002**, *102*, 4639–4750.
- (48) Lecaille, F.; Kaleta, J.; Brömme, D. *Chem. Rev.* **2002**, *102*, 4459–4488.
- (49) Seebach, D.; Aebi, J.; Wasmuth, D. *Organic Syntheses* **1985**, *63*, 109–120.

Table 1. Kinetic Parameters for Inhibition of Cathepsin B from Bovine Spleen by the Synthetic Inhibitors

inhibitor	K_i (μM)	k_{inact} (s^{-1}) $\times 10^3$	k_{inact}/K_i ($\text{M}^{-1}\text{s}^{-1}$) $\times 10^{-2}$
2 ^a	4.4 \pm 0.6	150 \pm 110	360 \pm 210
		3.4 \pm 0.7	7.7 \pm 1.9
15	7.3 \pm 0.8	3.6 \pm 0.4	4.9 \pm 0.8
		0.057 \pm 0.005	0.078 \pm 0.011
16	34 \pm 2	> 300	ND
		0.16 \pm 0.01	0.046 \pm 0.004
17	810 \pm 47	NI	

^a Kinetic parameters for inactivation of cathepsin B from human liver by inactivator **2**: $K_i = 3.2 \pm 0.4 \mu\text{M}$, $k_{\text{inact}} = (4.7 \pm 1.6) \times 10^{-2} \text{ s}^{-1}$ and $(3.9 \pm 2.3) \times 10^{-3} \text{ s}^{-1}$, k_{inact}/K_i $(1.5 \pm 0.5) \times 10^4 \text{ M}^{-1}\text{s}^{-1}$ and $(1.2 \pm 0.7) \times 10^3 \text{ M}^{-1}\text{s}^{-1}$. ND stands for “not determined”. NI stands for “no inactivation”.

to give **11**. A standard coupling of L-phenylalanine methyl ester with difluorobenzoyl chloride afforded compound **13**, which in turn resulted in **14** after the reaction with hydroxylamine. The coupling of **11** with **14** in the presence of PYBOP produced the desired compound **2**. That the acylation took place at the hydroxamic acid oxygen and not the nitrogen was confirmed by the ferric chloride test (5% $\text{FeCl}_3 \cdot 6\text{H}_2\text{O}$ in 0.5 N HCl).⁵⁰

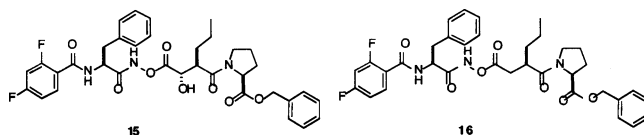
Compound **2** inhibited cathepsin B in a time-dependent manner, typical of covalent enzyme modifiers (Table 1). The kinetics of enzyme modification were biphasic, a rapid phase ($k_{\text{inact}} = 0.15 \pm 0.11 \text{ s}^{-1}$) preceded a slower one [$k_{\text{inact}} = (3.4 \pm 0.7) \times 10^{-3} \text{ s}^{-1}$]. The dissociation constant for the noncovalent pre-acylation complex of the inhibitor and enzyme, a measure of the affinity of the enzyme for the ligand, was determined at $K_i = 4.4 \pm 0.6 \mu\text{M}$ by a Dixon plot. The values for k_{inact}/K_i were calculated at $(3.6 \pm 2.1) \times 10^4 \text{ M}^{-1}\text{s}^{-1}$ and $(7.7 \pm 1.9) \times 10^2 \text{ M}^{-1}\text{s}^{-1}$ for the first and second phases, respectively. The process of inhibition is clearly favorable. We attempted to measure a rate constant for a potential recovery of enzyme activity (i.e., reversal of inhibition; k_{rec}), but such a measurement was not possible as recovery of activity was not detectable under these conditions. We allowed a portion of the enzyme to be inhibited completely and then dialyzed the sample overnight. Under these conditions, 5–6% of activity was recovered over the long duration. Therefore, the enzyme–inhibitor complex is stable. Furthermore, we investigated whether the process of enzyme inhibition also entailed any turnover of inhibitor **2** by measuring the partition ratio⁵¹ for the inhibitor. This experiment revealed that essentially one molecule of inhibitor **2** resulted in inhibition of one molecule of enzyme.

We also investigated the nature of the inhibited enzyme species by electrospray ionization mass spectrometry. Mass spectrometry revealed the formation of a 28 274 Da species on inhibition of the bovine cathepsin B, consistent with the incorporation of the entire structure of the inhibitor to the enzyme active site (an increase in mass of 708 Da; M+H). This finding is consistent with species **3** as the likely inhibited form of the enzyme. However, if the noncovalent fragment **5** were to be retained by the enzyme, the mass spectrometric result cannot preclude the formation of **4**, as the molecular mass for species **3**, and for **4** plus the retained fragment **5** are the same.

To explore if species **4** plus fragment **5** are formed on exposure of cathepsin B to **2**, we prepared a ¹³C version of inhibitor **2** in which the label was at the carbonyl carbon of the acetyl moiety. The synthesis was the same as in Scheme 2, except labeled acetic anhydride was used.

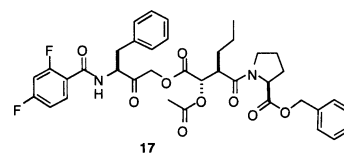
We incubated ¹³C-**2** (500 μM) with bovine cathepsin B (160 μM) in 300 μL of 50 mM MES buffer, 200 mM NaCl, 5 mM EDTA, 0.15% BRIJ 35, 1 mM DTT, and 1.5% DMSO-*d*₆, pH 6.0 at 4 °C in an NMR tube. A HMBC experiment was carried out,^{52,53} which revealed the presence of two acetyl signals, one at ¹³C NMR δ 172.6 and ¹H NMR δ 1.9 corresponding to ¹³C-**2** and another at ¹³C NMR δ 180.8 and ¹H NMR δ 1.7 corresponding to **5**. The former showed ¹³C coupling to the methine (¹H NMR δ 4.4) three bonds away in the inhibitor and the latter showed ¹³C coupling to the hydroxamate NH (¹H NMR δ 8.2), also three bonds away in species **5**. Therefore, it would appear that the interaction of inhibitor **2** with the cathepsin B active site does generate species **3** to give immediate inhibition of the enzyme, and over time release of compound **5** gives rise to species **4**, which is the ultimate inhibitory species.

The proposed mechanism of action of inhibitor **2** (Scheme 1) envisions that the acetoxyl moiety will interact with His-199. We evaluated the importance of the acetoxyl group for inhibition by synthesizing derivatives **15** and **16** (see Supporting Information).



It was interesting that both compounds **15** and **16** gave biphasic time-dependent inhibition of cathepsin B. However, they were both substantially poorer inhibitors compared to compound **2** (Table 1). They were also irreversible inhibitors of cathepsin B, which showed recoveries of activity of less than 2% after overnight dialysis of the inhibited enzyme samples. Both compounds also had poorer dissociation constants (K_i) compared to **2**. Since the hydroxyl moiety in **15** should still be able to hydrogen bond with His-199, its K_i was only 2-fold higher than that of **2**. In terms of k_{inact}/K_i , compound **2** was superior to both **15** and **16** by 2 to 4 orders of magnitude. Therefore, the acetoxyl group was clearly important for efficient inhibition of cathepsin B (effects on both K_i and k_{inact}), but not critical for the mode of inhibition.

The hydroxamate species of **2** would contribute to the favorable interactions with the active site in stabilizing the tetrahedral species **3**. To explore the contribution of the hydroxamate group to the inhibition process, we synthesized the carbon analogue, compound **17** (see Supporting Information). Compound **17** has all the features of inhibitor **2**, except its hydroxamate nitrogen was replaced by a carbon. Compound **17** was merely a poor noncovalent competitive inhibitor of cathepsin B, with a K_i of $810 \pm 47 \mu\text{M}$.



(50) Surman, M. D.; Mulvihill, M. J.; Miller, M. J. *J. Org. Chem.* **2003**, *67*, 4115–4121.

(51) Silverman, R. B. *Mechanism-Based Enzymes Inactivators: Chemistry and Enzymology*; CRC Press: Boca Raton, FL, 1988.

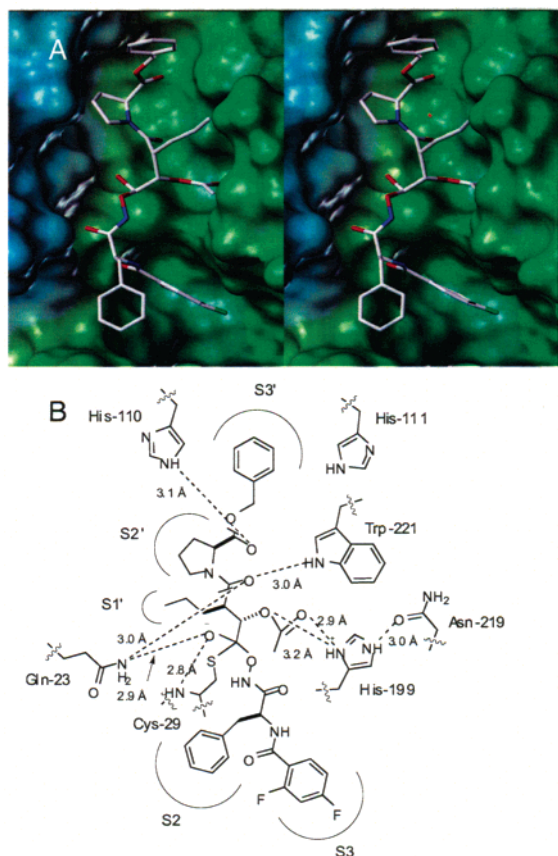


Figure 1. (A) A stereoview of the computational model for compound **2** bound to the active site of cathepsin B. A solvent-accessible surface was constructed for the active site. The ligand is shown in capped-sticks representation and color-coded according to atom types (white, blue, red, and green correspond to carbon, nitrogen, oxygen, and fluorine, respectively). (B) A schematic illustrating the various hydrogen bonding interactions of compound **2** with the enzyme. Distances correspond to mean values, which were determined by averaging over all the snapshots collected during the 960-ps simulation.

To further elucidate the structural bases for inhibition, a 960-ps molecular dynamics simulation of species **3** was carried out. The system was fully solvated and PME electrostatics were used to describe long-range electrostatics. The Cartesian coordinates from the last snapshot in the trajectory were used to illustrate the binding mode of **2** in the tetrahedral species, as shown in Figure 1A. The compound effectively exploits the primed and unprimed subsites of the active site. The propyl moiety at R_2 is pointing toward the S1' pocket of the enzyme, sharing the subsite with the acetoxy moiety of **2**. It is of interest to note that the acetoxy moiety forms hydrogen bonds with the N δ of His-199; both ester oxygens seem to be interacting with N δ of His-199 over the course of the trajectory, with mean distances of 3.2 and 2.9 Å, respectively (Figure 2A,B). Figure 2A shows that the hydrogen bond between N δ and the carbonyl oxygen experiences large fluctuations in the first 250 ps, but remains stable over the remainder of the trajectory. The other hydrogen bond—with the sp^3 hybridized oxygen of the ester moiety—is more stable as evidenced by the lack of large fluctuations in the distance (Figure 2B). These hydrogen bonds are thought to be the basis for the increase in efficiency of cathepsin B inactivation by compound **2**, compared to compounds **15** and **16**. It is interesting to note that in the period that the hydrogen bond to the carbonyl breaks (Figure 2A), there would appear

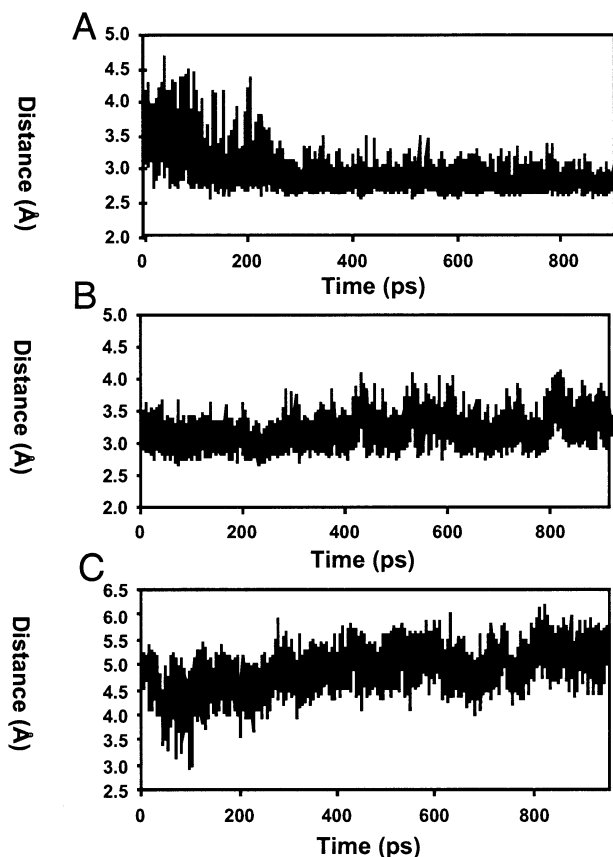


Figure 2. Distance from N δ of His-199 to (A) the ester oxygen carbonyl and (B) the sp^3 hybridized oxygen atom of the ester moiety and (C) to the charged oxygen of the tetrahedral species over the course of the 960 ps trajectory.

to be the opportunity for protonation of the tetrahedral species by His-199. The proline side chain binds into the S2' subsite, whereas the benzyl ester moiety points toward the S3' pocket, with its carbonyl forming a hydrogen bond with N δ of His-110. These two residues are thought to be the basis for efficient binding of the C-termini in substrates to the active site of cathepsin B. As shown in the schematic in Figure 1B, the oxygen of the tetrahedral species is ensconced into the oxyanion hole, forming hydrogen bonds with the backbone nitrogen of Cys-29 and the side-chain amide nitrogen of Gln-23, with mean distances of 2.8 and 3.0 Å, respectively.

The mechanism of inhibition of cathepsin B by nitrile-based inhibitors, which consist of the formation of a thioimidate as a result of proton transfer from the charged His-199 to the thioimide,⁵⁴ inspired the investigation of a similar event for species **3**. The distance from the charged oxygen of the tetrahedral species to the hydrogen at N δ was monitored over the course of the 960-ps trajectory and is shown in Figure 2. In a fleeting moment during the course of the trajectory (in the first 100 ps), the charged oxygen comes within hydrogen-bonding distance of N δ of His-199, making the proton migration from His-199 to the tetrahedral intermediate a possible event. *The resulting neutral species in the formation of species **3** may be plausible and might serve to stabilize the tetrahedral intermediate, which ultimately leads to species **4** in due course.*

In this manuscript, we have disclosed a novel class of irreversible inhibitors for cathepsin B, which is an important target for intervention of tissue invasiveness and metastasis of

cancer. The research benefited from computational methods and from syntheses of focused libraries of compounds that provided structural diversity. Compound **2** is the prototype of this type of cysteine protease inhibitor that should prove a new and useful tool in fighting cancer.

Experimental Section

(2R,3S)-Diisopropyl 2-allyl-3-hydroxysuccinate (6). A modified procedure described by Seebach was applied.⁴⁹ A 2.5 M solution of *n*-butyllithium (40 mL, 100 mmol) in hexane was added dropwise to a stirred solution of *N*-isopropylcyclohexylamine (16.8 mL, 102 mmol) and 2,2'-dipyridyl (107 mg, 0.69 mmol) in anhydrous THF (250 mL) at -75 °C. The reaction temperature was raised to -50 °C over 30 min. Diisopropyl (*S*)-malate (10.9 g, 50 mmol) in THF (20 mL) was added dropwise at -75 °C to the reaction mixture. The reaction flask was warmed to -50 °C over 1 h and then was cooled to -75 °C. A solution of 3-bromo-1-propene (8.65 mL, 100 mmol) in THF (10 mL) was added dropwise. Stirring was continued at -50 °C for 1 h, and then overnight while the temperature was raised to -5 °C. The reaction was quenched by addition of a solution of glacial acetic acid (12 g, 200 mmol) in diethyl ether (20 mL) at -50 °C and then poured into a mixture of ether (500 mL) and water (100 mL). The organic layer was washed with saturated NaHCO₃ and brine and dried over MgSO₄. The solvent was concentrated to dryness to give a crude product which was subjected to column chromatography (hexane:EtOAc = 10:1 ~ 6:1) yielding **6** as an oil (10.6 g, 82%); ¹H NMR (400 MHz, CDCl₃) δ 5.79 (m, 1H), 5.12 (m, 2H), 5.01 [m, 2H, OCH(CH₃)₂], 4.21 (dd, *J* = 6.4, 3.2 Hz, 1H, CHOH), 3.20 (d, *J* = 6.4 Hz, 1H, OH), 2.89 (m, 1H, CHCO₂R), 2.60 (m, 1H), 2.40 (m, 1H), 1.27 [dd, *J* = 6.0, 2.0 Hz, 6H, CH(CH₃)₂], 1.20 [d, *J* = 6.8 Hz, 6H, CH(CH₃)₂]; ¹³C NMR (100 MHz, CDCl₃) δ 173.3, 171.7, 135.3, 118.0, 70.5, 70.0, 68.8, 48.3, 32.5, 22.0, 21.9; HRMS (FAB) calcd for C₁₃H₂₃O₅ (MH⁺) 259.1545, found 259.1540.

(2R,3S)-2-Allyl-3-hydroxysuccinic Acid (7). 2 N KOH (20 mL, 40 mmol) was added to a solution of **6** (3.20 g, 12.3 mmol) in 1:1 THF-MeOH (20 mL). The reaction mixture was stirred at room temperature for 24 h. The volume was reduced by approximately 60% under reduced pressure. The residue was acidified to pH 1 with 6 N HCl and was saturated with NaCl. The resultant aqueous solution was washed with EtOAc (5 \times). The combined organic layers were dried over MgSO₄, filtered, and concentrated to dryness. Recrystallization from ether/pentane gave **7** (1.88 g, 88%) as a white solid. mp 91–93 °C; ¹H NMR (500 MHz, CD₃OD) δ 5.84 (m, 1H), 5.09 (m, 2H), 4.90 (br, 3H), 4.25 (d, *J* = 5.0 Hz, 1H, CHOH), 2.90 (m, 1H, CHCO₂R), 2.50 (m, 1H), 2.35 (m, 1H); ¹³C NMR (125 MHz, CD₃OD) δ 175.2, 174.3, 135.5, 116.4, 70.4, 48.8, 32.2; MS (EI) 197.04 (M + Na⁺), 192.08, 175.04, 129.04.

2(R)-[2,2-Dimethyl-5-oxo-(1,3)dioxolan-4(S)-yl]-pent-4-enoic Acid (8). Compound **7** (1.81 g, 10.4 mmol) in dimethoxypropane (10 mL) was treated with TsOH (100 mg, 0.6 mmol). The reaction mixture was stirred at room-temperature overnight, after which it was concentrated to dryness. The residue was diluted with EtOAc (40 mL) and was washed with water and brine. The organic layer was dried over MgSO₄, filtered, and concentrated, giving a crude product which was subjected to column chromatograph (CH₂Cl₂:MeOH:AcOH = 300:5:1) to afford **8** (1.71 g, 77%) as an oil; ¹H NMR (400 MHz, CDCl₃) δ 5.78 (m, 1H), 5.17 (m, 2H), 4.51 (d, *J* = 4.0 Hz, 1H, CHOR), 3.05 (m, 1H, CHCO₂H), 2.70 (m, 1H), 2.49 (m, 1H), 1.59 (s, 3H), 1.53 (s, 3H); ¹³C NMR (100 MHz, CDCl₃) δ 176.8, 172.1, 134.2, 118.9, 111.5, 73.2, 46.5, 32.0, 26.7, 26.3.

2(R)-[2,2-Dimethyl-5-oxo-(1,3)dioxolan-4(S)-yl]-pentanoic Acid (9). A solution of **8** (0.88 g, 4.11 mmol) in MeOH (20 mL) was charged with activated carbon (150 mg, 10%). The mixture was stirred at room-temperature overnight under an atmosphere of hydrogen. After filtration, the filtrate was concentrated to dryness to give **9** (0.89 g, quantitative);

¹H NMR (500 MHz, CDCl₃) δ 4.49 (d, *J* = 4.5 Hz, 1H, CHOR), 2.91 (m, 1H, CHCO₂H), 1.84 (m, 1H), 1.75 (m, 1H), 1.60 (s, 3H), 1.54 (s, 3H), 1.43 (m, 2H), 0.95 (t, *J* = 7.3 Hz, 3H, CH₂CH₃); ¹³C NMR (125 MHz, CDCl₃) δ 176.7, 172.4, 111.3, 74.2, 47.1, 29.9, 26.8, 26.4, 20.7, 14.1; HRMS (FAB) calcd for C₁₀H₁₇O₅ (MH⁺) 217.1076, found 217.1058.

1-[2(R)-(2,2-Dimethyl-5-oxo-[1,3]dioxolan-4(S)-yl)-pentanoyl]-proline Benzyl Ester (10). The acid **9** (1.54 g, 7.1 mmol), PYBOP (3.64 g, 7.0 mmol) and 1-hydroxy-7-azabenzotriazole (0.95 g, 7.0 mmol) were dissolved in anhydrous DMF (15 mL). L-ProObn·HCl (1.72 g, 7.1 mmol) was added to the reaction mixture at -10 °C, followed by dropwise addition of DIPEA (2.47 mL, 14.2 mmol) over 5 h. After 18 h, the residue was diluted with EtOAc (40 mL). The organic layer was washed with brine (20 mL) and saturated aqueous NaHCO₃ (20 mL), dried over MgSO₄, filtered, and evaporated. The crude product was purified by column chromatograph (hexane:EtOAc = 2:1 ~ 3:2) to afford **10** (2.21 g, 78%) as an oil; ¹H NMR (500 MHz, CDCl₃) δ 7.33 (m, 5H, Ph), 5.15 (q, *J* = 12.0 Hz, 2H, OCH₂Ph), 4.63 (dd, *J* = 8.5, 4.0 Hz, 1H, CHCO₂Bn), 4.52 (d, *J* = 9.5 Hz, 1H, CHOR), 3.64 (m, 2H, CH₂NR₂), 2.95 (td, *J* = 9.5, 4.5 Hz, 1H, CHPr), 2.20 (m, 1H, CH₂CHCO₂Bn), 1.98 (m, 4H), 1.77 (m, 1H, CH₂Et), 1.60 [s, 3H, C(CH₃)₂], 1.51 [s, 3H, C(CH₃)₂], 1.48 (m, 1H, CH₂CH₃), 1.28 (m, 1H, CH₂CH₃), 0.83 (t, *J* = 7.3 Hz, 3H, CH₂CH₃); ¹³C NMR (125 MHz, CDCl₃) δ 172.4, 172.1, 171.1, 135.9, 128.8, 128.4, 128.3, 110.7, 74.5, 67.0, 59.1, 47.6, 46.4, 30.2, 29.4, 27.3, 26.1, 25.0, 20.0, 14.4.

1-[2(R)-((S)-Acetoxy-carboxy-methyl)-pentanoyl]-proline Benzyl Ester (11). A solution of **10** (0.57 g, 1.4 mmol) in THF (2 mL), *t*-BuOH (1 mL) and 1 N HCl (2 mL) was stirred at 4 °C overnight. The solvent was removed to dryness under reduced pressure. The residue was dissolved in dichloromethane (10 mL) and was treated with pyridine (178 mL, 2.2 mmol) and acetic anhydride (198 mL, 2.1 mmol). The resulting solution was stirred at room temperature for 6 h. The solvent was concentrated to dryness to give a crude product, which was subjected to column chromatography (CH₂Cl₂:MeOH:AcOH = 120:5:1 ~ 60:5:1) giving the pyridinium salt of **11** as an oil (0.63 g, 93%); ¹H NMR (500 MHz, CDCl₃) δ 8.64 (d, *J* = 4.5 Hz, 2H, pyr), 7.83 (m, 1H, pyr), 7.42 (m, 2H, pyr), 7.30 (m, 5H, Ph), 5.13 (dd, *J* = 38.5, 12.0 Hz, 2H, OCH₂Ph), 5.13 (d, *J* = 6.0 Hz, 1H, CHOAc), 4.60 (dd, *J* = 8.5, 4.0 Hz, 1H, CHCO₂Bn), 3.74 (m, 1H, CH₂NR₂), 3.64 (m, 1H, CH₂NR₂), 3.04 (m, 1H, CHPr), 2.22 (m, 1H), 2.04 (s, 3H, Ac), 1.99 (m, 3H), 1.68 (m, 1H), 1.60 (m, 1H), 1.43 (m, 1H), 1.32 (m, 1H), 0.83 (t, *J* = 12.5 Hz, 3H, CH₂CH₃); ¹³C NMR (125 MHz, CDCl₃) δ 173.2, 171.5, 170.9, 170.1, 147.3, 138.9, 135.6, 128.8, 128.6, 128.4, 124.9, 73.4, 67.3, 59.5, 48.1, 45.0, 31.0, 29.4, 25.0, 20.9, 20.4, 14.3; HRMS (FAB) calcd for C₂₁H₂₈N₂O₇ (MH⁺) 406.1866, found 406.1891.

(S)-2,4-Difluorobenzoylphenylalanine Methyl Ester (13). The title compound was prepared by a modified method of Fitt and co-workers.⁵⁵ Sodium 2-ethylhexanoate (6.65 g, 40 mmol) was added to a suspension of phenylalanine methyl ester hydrochloride (4.31 g, 20 mmol) in THF (40 mL). After being stirred at room temperature for 1 h, 2,4-difluorobenzoyl chloride (2.58 mL, 21 mmol) was added to the solution at -10 °C. After 3 h, the residue was diluted with EtOAc (200 mL) and was washed with saturated NaHCO₃ (100 mL \times 3) and brine (60 mL). The organic layer was dried over MgSO₄, filtered, and concentrated. The product was purified by silica gel chromatography (hexane:EtOAc = 5:1 ~ 3:1) to afford **13** (6.13 g, 96%) as an oil; ¹H NMR (500 MHz, CDCl₃) δ 8.08 (q, *J* = 8.2 Hz, 1H), 7.27 (m, 3H), 7.16 (dd, *J* = 3.5, 1.5 Hz, 2H), 7.09 (m, 1H, NHCO), 6.97 (m, 1H), 6.46 (ddd, *J* = 11.0, 8.5, 2.5 Hz, 1H), 5.06 (qd, *J* = 8.0, 2.0 Hz, 1H, CHCO₂Me), 3.75 (s, 3H, OCH₃), 3.23 (qd, *J* = 14.0, 6.0 Hz, 2H, CHCH₂Ph); ¹³C

(52) Bax, A.; Summers, M. F. *J. Am. Chem. Soc.* **1986**, *108*, 2093–2094.

(53) Martin, G. E.; Zektzer, A. S. *Two-Dimensional NMR Methods for Establishing Molecular Connectivity*; VCH: Weinheim, 1988.

(54) Brisson, J. R.; Carey, P. R.; Storer, A. C. *J. Biol. Chem.* **1986**, *261*, 9087–9089.

(55) Fitt, J.; Prasad, K.; Repic, O.; Blacklock, T. J. *Tetrahedron Lett.* **1998**, *39*, 6991–6992.

NMR (125 MHz, CDCl₃) δ 171.9, 165.2 (dd, $J = 256.2$, 13.1 Hz, CF), 162.1 (d, $J = 2.8$ Hz, CO), 161.3 (dd, $J = 251.6$, 13.1 Hz, CF), 135.9, 134.0 (dd, $J = 10.2$, 3.8 Hz), 129.5, 128.9, 127.5, 117.2 (dd, $J = 11.2$, 3.8 Hz, q), 112.6 (dd, $J = 21.4$, 2.8 Hz), 104.6 (dd, $J = 27.9$, 26.0 Hz), 54.2, 52.6, 38.1; HRMS (FAB) calcd for C₁₇H₁₆F₂N₃O₃ (MH⁺) 320.1098, found 320.1112.

(S)-2,4-Difluorobenzoyl-phenylalanine N-Hydroxyamide (14). The synthesis was carried out according to a modified procedure of Ritter.⁵⁶ A solution of **13** (3.46 g, 10.8 mmol) in methanol (20 mL), cooled in an ice bath, was charged with a preformed slurry of hydroxylamine hydrochloride (1.39 g, 20 mmol) and KOH (2.24 g, 40 mmol). The reaction mixture was stirred under argon overnight and then was acidified to an apparent pH of 4 with concentrated HCl. The solvent was removed under reduced pressure to give a white solid. The solid was repeatedly boiled in ethyl acetate and filtered until TLC analysis revealed that no ferric chloride-positive component remained in the filtrate. The combined filtrate was concentrated under reduced pressure to yield **14** (3.42 g, 99%) as a white powder; ¹H NMR (500 MHz, CD₃OD) δ 7.70 (q, $J = 8.0$ Hz, 1H), 7.27 (m, 3H), 7.21 (m, 2H), 7.03 (m, 2H), 4.86 (s, 3H), 4.73 (t, $J = 7.5$ Hz, 1H, CHCH₂Ph), 3.16 (dd, $J = 13.5$, 7.0 Hz, 1H, CHCH₂Ph), 3.04 (dd, $J = 14.0$, 8.0 Hz, 1H, CHCH₂Ph); ¹³C NMR (125 MHz, CD₃OD) δ 168.8, 164.9 (dd, $J = 253.5$, 12.1 Hz, CF), 164.0, 160.9 (dd, $J = 252.5$, 12.1 Hz, CF), 136.8, 132.3 (dd, $J = 10.2$, 3.6 Hz), 129.2, 128.4, 126.8, 118.9 (d, $J = 14.7$ Hz, q), 111.7 (dd, $J = 22.2$, 3.8 Hz), 104.3 (t, $J = 27.0$ Hz), 53.2, 38.0; HRMS (FAB) calcd for C₁₆H₁₅F₂N₂O₃ (MH⁺) 321.1051, found 321.1074.

1-(2(R)-{1(S)-acetoxy-2-[2(S)-(2,4-difluoro-benzoylamino)-3-phenylpropionylaminoxy]-2-oxo-ethyl}-pentanoyl)-pyrrolidine-2(S)-carboxylic Acid Benzyl Ester (2). Diisopropylethylamine (409 μ L, 2.35 mmol) was added dropwise to a mixed solution of acid **11** (940 mg, 2.32 mmol), hydroxyamide **14** (288 mg, 0.90 mmol), and PYBOP (1.21 g, 2.32 mmol) in DMF (20 mL) at -10 °C over 8 h. The reaction mixture was stirred at room-temperature overnight. An additional amount of diisopropylethylamine (208 μ L, 1.20 mmol) was added dropwise to the reaction mixture over 4 h. After an additional 3 h, the solvent was evaporated under reduced pressure. Column chromatography (CHCl₃:EtOH:AcOH = 60:1:0.2) afforded the title compound (1.29 g, 78%); ¹H NMR (500 MHz, CDCl₃) δ 8.03 (m, 1H), 7.37–7.21 (m, 11H), 7.11 (dd, $J = 12.5$, 7.0 Hz, 1H), 6.97 (m, 1H), 6.84 (m, 1H), 5.16 (q, $J = 13.5$ Hz, 2H, OCH₂Ph), 5.10 (d, $J = 10.0$ Hz, 1H, CHOAc), 4.96 (m, 1H, CHCH₂Ph), 4.61 (dd, $J = 8.5$, 4.5 Hz, 1H, CHCO₂Bn), 3.76 (m, 1H, CH₂NR₂), 3.68 (m, 1H, CH₂NR₂), 3.30 (dd, $J = 14.0$, 6.5 Hz, 1H, CHCH₂Ph), 3.19 (dd, $J = 14.5$, 8.5 Hz, 1H, CHCH₂Ph), 3.15 (m, 1H, CHPr), 2.22 (m, 1H), 2.08–1.95 (m, 3H), 2.05 (s, 3H, ROCOCH₃), 1.75 (m, 2H, CH₂Et), 1.48 (m, 1H, CH₂-CH₃), 1.27 (m, 1H, CH₂CH₃), 0.87 (t, $J = 7.3$ Hz, 3H, CH₂CH₃); ¹³C NMR (125 MHz, CDCl₃) δ 171.9, 170.6, 170.2, 168.5, 167.7, 165.5 (dd, $J = 256.2$, 12.1 Hz, CF), 163.3, 161.4 (dd, $J = 251.6$, 12.9 Hz, CF), 135.8, 134.1 (dd, $J = 10.2$, 3.3 Hz), 129.6, 129.0, 128.8, 128.5, 128.4, 127.5, 116.5 (d, $J = 11.2$ Hz, q), 112.8 (d, $J = 21.4$ Hz), 104.7 (dd, $J = 28.8$, 26.0 Hz), 73.4, 67.1, 59.3, 52.7, 47.7, 44.9, 37.5, 30.2, 29.5, 25.1, 20.6, 19.9, 14.3; HRMS (FAB) calcd for C₃₇H₄₀F₂N₃O₉ (MH⁺) 708.2733, found 708.2759.

Kinetic Determinations. The fluorometric activity assays were carried out by monitoring hydrolysis of Z-Phe-Arg-7-amido-4-methylcoumarin hydrochloride (Z-Phe-Arg-AMC, Sigma) at room temperature for cathepsin B from bovine spleen (Sigma), with excitation wavelength of 380 nm and emission wavelength of 460 nm. The assay mixture was comprised of 50 mM MES, 200 mM NaCl, 5 mM EDTA, 0.15% BRIJ 35, 1 mM DTT, pH 6.0 at 20 °C. These experiments were performed under conditions of excess substrate concentrations.⁵⁷

The dissociation constants (K_i) were calculated by the method of Dixon.⁵⁸ Two concentrations of Z-Phe-Arg-AMC were used (2 μ M and

6 μ M) and the concentrations of inhibitors were varied from 0 to 80 μ M. Enzyme concentration in the assays was 3 nM.

Initial rates of inactivation (k_{inact}) were measured as described by Silverman.⁵¹ A series of inactivation experiments were carried out with inactivator concentrations within the range of 1 to 80 μ M. Typically, a solution of inactivator in DMF was added to an enzyme solution in the above-mentioned assay mixture to afford a final concentration of 0.70 μ M enzyme in 1.2% DMF for a given inactivator concentration. The solutions were incubated at 0 °C. Every few minutes, 30 μ L samples of the inactivation mixture were removed and added to 570 μ L of the assay buffer containing 6 μ M of Z-Phe-Arg-AMC and the increase in the emission fluorescence at 460 nm was monitored for the first 30 s of the reaction immediately.

The partition ratio was evaluated by the titration method.⁵¹ A series of solutions (200 μ L each), containing 0.4 μ M enzyme and various molar equivalents of inhibitor **2**, were prepared to give [I]₀/[E]₀ ratios of 0.01 to 5 in 50 mM MES buffer, 200 mM NaCl, 5 mM EDTA, 1 mM DTT, and 1% DMSO, pH 6.0 and the solutions were incubated at 4 °C for 15–17 h. Subsequently, 50 μ L samples of each solution were added to 550 μ L of the above-mentioned assay mixture containing 10 μ M of Z-Phe-Arg-AMC (Sigma) and the activities were measured immediately. Control experiments were carried out in the same manner in the absence of the inhibitor.

Sample preparation for Mass Spectrometry of the Enzyme–Inhibitor Complex. Cathepsin B from bovine spleen (Sigma, 75 μ g, 2.73 nmol) was dissolved in 200 μ L of an assay buffer containing 50 mM MES, 200 mM NaCl, 5 mM EDTA, 0.15% BRIJ 35, 1 mM DTT, pH 6.0 at 4 °C, and then a 32 mM DMF solution of inhibitor **2** (4 μ L, 128 nmol) was added to the mixture. After 2 h, when the enzyme was inhibited completely, the enzyme–inhibitor complex was dialyzed at 4 °C against distilled water (4 \times 800 mL) over 24 h. The solution was concentrated to 40 μ L using centrifugal filtration (Ultrafree-4, Millipore) to give 68- μ M enzyme. A control experiment was carried out in the exact same manner, except no inhibitor was added to the enzyme solution.

Computational Procedures. The X-ray structure of an acyl-enzyme complex provided the initial coordinates for the molecular dynamics simulations (RCSB code IGMV). Crystallographic waters were retained and hydrogen atoms were added to the protein using the “Protonate” program, which is part of the AMBER 7⁵⁹ suite of programs. AMBER force field parameters and atomic charges were assigned to all atoms using the parm99 set of parameters. The Sybyl program (Tripos Inc., St. Louis, MO) was used for the manipulation and visualization of all structures and for the protonation of the bound ligand. The atomic charges of the bound ligand were determined using the RESP methodology.⁶⁰ This consisted of first optimizing the molecules using HF/6-31G*, followed by a HF/6-31G* single-point energy calculation to determine the electrostatic potential around the molecule, which was subsequently used in the two-stage RESP fitting procedure. The

(58) Dixon, M. *Biochem. J.* **1953**, *55*, 170–171.

(59) Case, D. A.; Pearlman, D. A.; Caldwell, J. W.; Cheatham III, T. E.; Wang, J.; Ross, W. S.; Simmerling, C. L.; Darden, T. A.; Merz, K. M.; Stanton, R. V.; Cheng, A. L.; Vincent, J. J.; Crowley, M.; Tsui, V.; Gohlke, H.; Radmer, R. J.; Duan, Y.; Pitera, J.; Massova, I.; Seibel, G. L.; Singh, U. C.; Weiner, P. K.; Kollman, P. A.; AMBER 7 ed.; University of California: San Francisco, 2002.

(60) Bayly, C. I.; Cieplak, P.; Cornell, W. D.; Kollman, P. A. *J. Phys. Chem.* **1993**, *97*, 10 269–10 280.

(61) Frisch, M. J.; Trucks, G. W.; Schlegel, H. B.; Scuseria, G. E.; Robb, M. A.; Cheeseman, J. R.; Zakrzewski, V. G.; Montgomery Jr., J. A.; Stratmann, R. E.; Burant, J. C.; Dapprich, S.; Millam, J. M.; Daniels, A. D.; Kudin, K. N.; Strain, M. C.; Farkas, O.; Tomasi, J.; Barone, V.; Cossi, M.; Cammi, R.; Mennucci, B.; Pomelli, C.; Adamo, C.; Clifford, S.; Ochterski, J.; Petersson, G. A.; Ayala, P. Y.; Cui, Q.; Morokuma, K.; Malick, D. K.; Rabuck, A. D.; Raghavachari, K.; Foresman, J. B.; Cioslowski, J.; Ortiz, J. V.; Stefanov, B. B.; Liu, G.; Liashenko, A.; Piskorz, P.; Komaromi, I.; Gomperts, R.; Marti, R. L.; Fox, D. J.; Keith, T.; Al-Laham, M. A.; Peng, C. Y.; Nanayakkara, A.; Gonzalez, C.; Challacombe, M.; Gill, P. M. W.; Johnson, B.; Chen, W.; Wong, M. W.; Andres, J. L.; Gonzalez, C.; Head-Gordon, M.; Replogle, E. S.; Pople, J. A.; Gaussian Inc.: Pittsburgh, PA, 1998.

(56) Ritter, A. R.; Miller, M. J. *J. Org. Chem.* **1994**, *59*, 4602–4611.

(57) Koerber, S. C.; Fink, A. L. *Anal. Biochem.* **1987**, *165*, 75–87.

Gaussian 98 package⁶⁰ was used to carry out all ab initio calculations. The acyl-enzyme complex was immersed in a box of TIP3P⁶² water molecules such that no atom in the acyl-enzyme complex was within 12 Å from any side of the box; after solvation of the acyl-enzyme complex, the system consisted of a total of 65071 atoms. All bonds involving hydrogen atoms were constrained using the SHAKE algorithm and a 2-fs time step was used. The particle mesh Ewald⁶³ method was used to treat long-range electrostatics. Water molecules were first energy-minimized and equilibrated by running a short simulation with the acyl-enzyme species fixed using Cartesian restraints. This was followed by a series of energy minimizations, where the Cartesian restraints were gradually relaxed from 500 kcal/Å² to 0 kcal/Å² and the system was subsequently slowly heated to 300 K via a 300 ps molecular dynamics run. Another 50 ps simulation was carried out at 300 K for further equilibration. A 960-ps simulation at constant pressure and temperature (1 atm and 300 K, respectively) was then carried out on a 1.533 GHz Athlon processor cluster with a Myrinet switch. Snapshots were collected every 0.2 ps.

(62) Jorgensen, W. L.; Chandrasekhar, J.; Madura, J. D.; Impey, R. W.; Klein, M. L. *J. Chem. Phys.* **1983**, *79*, 926–935.

(63) Darden, T. A.; York, D. M.; Pedersen, L. G. *J. Chem. Phys.* **1993**, *98*, 10 089–10 092.

As compounds were designed over the course of this study, they were systematically docked into the active site of cathepsin B using a Lamarckian genetic algorithm as implemented in the AutoDock 3.04³⁸ program. Sybyl was used to protonate the protein and charges were assigned using Sybyl's Kollman charges. AM1-BCC charges were assigned to the ligand using the antechamber module of the AMBER package. Parameters for the docking runs were similar to those used previously, except for the following differences:³⁸ the quaternion step, the translation step, and the torsion step were set to 0.2, 5, and 5, respectively. The number of evaluations was increased to 2.5×10^6 and the ligand was fully flexible during the docking runs.

Acknowledgment. This work was supported by Grant No. DAMD17-00-1-0496 from the U.S. Army.

Supporting Information Available: **Supporting Information Available:** Synthetic protocols and characterization of intermediates leading to compounds **15**, **16**, and **17** (PDF). This material is available free of charge via the Internet at <http://pubs.acs.org>.

JA0489240